NUMERICAL SIMULATION OF TRANSITION TO DETONATION IN A HYDROGEN-AIR MIXTURE DUE TO SHOCK WAVE FOCUSING ON A 90-DEG WEDGE

Bermudez De La Hoz, J.[1], Rudy, W.[2], Khair Allah, S.[3] and Teodorczyk, A.[4]

[1] Institute of Heat Engineering, Warsaw University of Technology, Nowowiejska 21/25, 00-665, Warsaw, Poland, jose.bermudez_de_la_hoz.dokt@pw.edu.pl
[2] Institute of Heat Engineering, Warsaw University of Technology, Nowowiejska 21/25, 00-665, Warsaw, Poland, wojciech.rudy@pw.edu.pl
[3] Institute of Heat Engineering, Warsaw University of Technology, Nowowiejska 21/25, 00-665, Warsaw, Poland, shamma.khair_allah.dokt@pw.edu.pl
[4] Institute of Heat Engineering, Warsaw University of Technology, Nowowiejska 21/25, 00-665, Warsaw, Poland, andrzej.teodorczyk@pw.edu.pl

ABSTRACT

The interaction of a shock wave with a specific angle or concave wall due to its reflection and focusing is a way to onset the detonation provided sufficiently strong shock wave. In this work, we present numerical simulation results of the detonation initiation due to the shock reflection and focusing in a 90-degree wedge for mixtures of H_2 and air. The code used was ddtFoam [1–3] that is a component of the larger OpenFOAM open-source CFD package of density-based code for solving the unsteady, compressible Navier-Stokes equations. The numerical model represents the 2-D geometry of the experiments performed by Rudy [4]. The numerical results revealed three potential scenarios in the corner after reflection: shock wave reflection without ignition, deflagrative ignition with intermediate transient regimes with a delayed transition to detonation in lagging combustion zone at around 1.8 mm from the apex of the wedge, and ignition with an instantaneous transition to detonation with the formation of the detonation wave in the corner tip. In the experimental investigation, the transition velocity for the stoichiometric mixture was approximately 715 m/s, while in the numerical simulation, the transition velocity for the stoichiometric mixture was 675.65 m/s, 5.5% decrease in velocity.

1. INTRODUCTION

Hydrogen has gained significant interest across various industries as a sustainable and eco-friendly alternative to traditional energy sources, mainly due to its highly reactive nature and carbon-free combustion process resulting in water vapour. Despite extensive research into the combustion of hydrogen, numerous unresolved issues remain. The potential for unforeseen explosions presents a serious safety concern in hydrogen production, transportation, storage, and consumption facilities. If hydrogen accidentally leaks in an enclosed space, it could produce flammable mixtures that, with even a minor ignition source, could result in unintended deflagration, posing a significant risk to nearby individuals and surrounding facilities. The severity of the consequences depends on the propagation speed of the deflagration.

The hazardous potential of a detonation, especially during the unsteady transition process, far outweighs that of a deflagration. As a result, a considerable amount of research has been devoted to examining the characteristics of accelerating deflagrations and identifying the conditions that lead to successful deflagration-to-detonation transitions (DDTs) in industrial settings to address safety concerns. Concurrently, detonation can be utilised in propulsion systems due to the high heat release rate, providing higher thermal efficiency than rocket or turbine engines. Pulse detonation engines (PDEs) and rotating detonation engines (RDEs) appear to be the most promising types of detonation-driven propulsion.

Research on deflagration-to-detonation transitions has a long development history, with numerous studies focusing on accelerating the flame by increasing turbulence through introducing various turbulators, such as Shchelkin spirals, perforated plates, multiple barriers, and complex geometries.

However, an alternative approach to initiating detonation involves the interaction and merging of a planar incident shock wave reflection from a concave wall or a specific angle, which then converges towards the focus of the reflector cavity. This phenomenon, known as shock focusing, occurs when shock waves merge into a small region, creating high pressure and temperature conditions that are highly favourable for detonation initiation in a combustible mixture.

There are several works devoted to numerical and experimental research of detonation onset due to shock focusing [5–12], however, the current study aimed to gather essential data on the transition to detonation by shock reflection on a 90-degree wedge for different concentrations of hydrogen in air mixtures at initial pressure of 1 bara.

2. MODEL DESCRIPTION

The 2D geometry of the experiments conducted by Rudy [4] (shown in Fig. 1) was represented by a numerical model. The computational domain emulated the final segment of a 0.11 x 0.11 x 2 m tube used in the experiments (as shown in Fig. 2). A customized end section was incorporated into the tube, which provided a cavity with an opening angle of 90°. The tube was filled with a hydrogen-air mixture. The numerical domain is a standard shock tube case, consisting of high-pressure (8-15 bar, 298 K) and low-pressure (1 bar, 298 K) sections to generate a planar shock wave approaching the wedge at the end of the tube at a specific velocity. The shock wave reflected from the wedge, and the accompanying focusing processes were analysed. The gases were at rest before the start of the calculations, and the shock wave was initiated at the outset of the simulation, with a leading velocity ranging from approximately 600 to 900 m/s. In the experiments by Rudy [4] the leading shock wave was generated by ignition and flame acceleration in the initial part of the tube. The further part of the tube was used to lead the leading shock wave stabilize.

The numerical simulation employed a mesh comprising two parts: one structured and orthogonal, while the other unstructured, containing approximately 50,300 cells between them. A total of 60 simulations were conducted with various hydrogen in air concentrations ranging from 15% to 50%, corresponding to an equivalence ratio of 0.42 to 2.91. The initial temperature and pressure were set to 293 K and 101,325 Pa, respectively, while the walls were assumed to be non-slip and adiabatic. To resemble the experimental setup, numerical sensors measuring temperature and pressure were placed at the same location as in the experiments during the simulations.

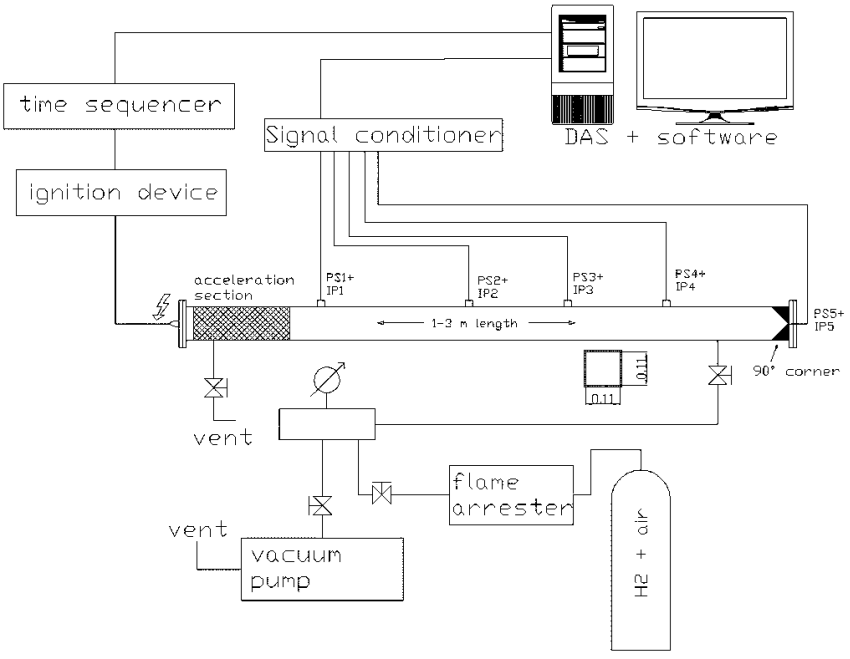

Figure 1. Experimental setup scheme performed by Rudy [4].

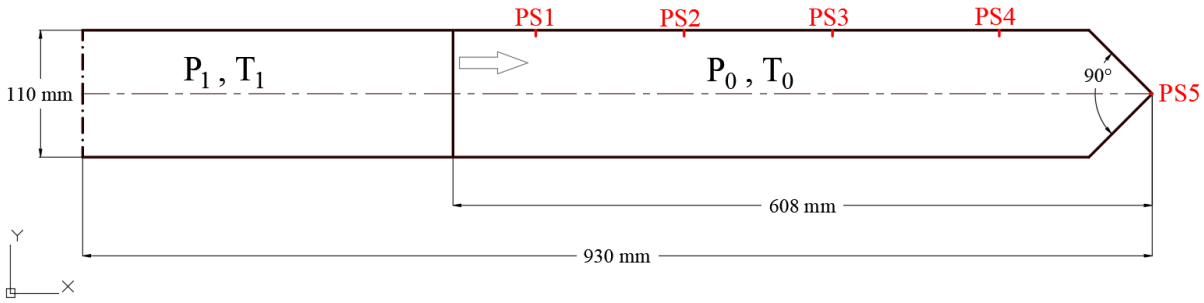

Figure 2. Sketch of computational domain (only half being simulated due to symmetry).

3. NUMERICAL METHODOLOGY

The ddtFoam solver from the OpenFOAM® toolbox developed by Ettner et al. [1–3] was used. The solver, which is density-based, has the ability to simulate various phenomena such as deflagration-to-detonation transition, flame acceleration, and detonation propagation in a single run. DdtFoam solves the unsteady, compressible Navier-Stokes equations equipped for high Mach number compressible flows shock capturing with the HLLC scheme to determine all the convective fluxes [3, 13]. This scheme produces accurate shock propagation speeds and less dissipation at discontinuities than standard schemes used in most pressure-based codes like the PISO scheme [14]. The solver is computationally efficient as both deflagration and detonation are described using a reaction progress variable, with combustion modelled with the Weller gradient combustion model [15] and autoignition delay time using O'Conaire's reaction scheme mechanism [16]. To avoid calculating ignition delay time in every time step and computational cell, the solver uses a pre-calculated table of ignition delay time (IDT) prepared with Cantera software. The IDT table is accessed during the simulation, and the solver compares the tabulated IDT with the simulated fluid residence time at specific conditions. If the residence time exceeds the precalculated IDT value, the solver activates the second source term in the reaction progress transport equation, significantly reducing the numerical cost of simulation. The solver is applicable to unstructured grids and works on relatively coarse grids making it suitable for intricate geometries. Realistic material properties for the reacting hydrogen-air mixture are obtained from the Chemkin database [17].

The Navier-Stokes equations, along with energy and species conservation equations that describe fluid motion, are solved using the finite volume method on a computational grid. These equations include:

1. Continuity equation:

$$\frac{\partial \rho}{\partial t} + \nabla \cdot (\rho u) = 0 \tag{1}$$

where ρ is the density and u is the velocity vector.

2. Momentum equation:

$$\frac{\partial (\rho u)}{\partial t} + \nabla \cdot (\rho u u) = -\nabla p + \nabla \cdot \tau + \rho g \tag{2}$$

where p is the pressure, τ is the viscous stress tensor, and g is the gravitational acceleration vector.

3. Energy equation:

$$\frac{\partial (\rho E)}{\partial t} + \nabla \cdot \big((\rho E + p) u\big) = -\nabla \cdot q + \nabla \cdot (\tau u) + \dot{Q} \tag{3}$$

where E is the total energy per unit mass, q is the heat flux vector, and $\dot{Q}$ is the rate of heat release due to chemical reactions.

4. Species transport equation:

$$\frac{\partial(\rho Y_k)}{\partial t} + \nabla \cdot (\rho Y_k u) = \nabla \cdot (\rho D(\nabla Y_k)) + \dot{\omega}_k \quad (4)$$

where Y_k is the mass fraction of species k, D is the diffusion coefficient and $\dot{\omega}_k$ is the net rate of production of species k due to chemical reactions.

In addition to these equations, ddtFoam integrates models for turbulence and heat transfer, and the k-ω SST (Shear Stress Transport) turbulence model was selected for turbulence modelling. This modelling strategy merges the benefits of k-ε and k-ω, as it behaves like k-ω in regions close to walls and switches to k-ε in a free stream region.

4. RESULTS AND DISCUSSION

The numerical results were processed similarly to experiments [4] by recording indications from pressure sensors using the Time of Arrival method to extract the velocity profiles of the shock wave along the tube. Three ignition modes were observed, shown in Figs. 3 to 5, similar to the experiment results obtained by Li and Zhang [11] and Yang and Zhang [12]. The first mode being peak local ignition mode (PLIM), involved a deflagrative ignition in the corner, similar to the "weak" ignition mode, occurring at lower velocities. The second mode being boundary ignition mode (BIM), involved deflagrative ignition with transition to detonation delayed by 301-647 μs after reflection. The third, strong ignition mode (SIM), involved direct transition to detonation in the corner, with ignition delay time lower than 12 μs.

Figure 3 corresponds to PLIM. In this case, the flame is generated at the apex of the wedge-shaped reflector but propagates slowly and concentrates on the apex for a long time. Observations show that at 0.89 ms incident shock that comes from the middle of the view field is reflected to produce two symmetrical R1 shock waves. At 0.995 ms, a flame core appears at the reflector's apex, and a second shock wave propagates from the peak of the wedge. By 1.095 ms, shock waves have integrated, and a third shock wave is observed propagating laterally generated by the second shock wave passing through the junction of the reflector's edge and the tube wall. At 1.165 ms, the flame still only spreads slowly in the wedge reflector.

Figure 4 illustrates BIM, where the flame is firstly generated at the apex of the wedge and then propagates along the tube wall. Initially, it resembles the peak local ignition mode, and at 0.93 ms, a flame kernel appears at the apex of the wedge and spreads slowly. By 1.25 ms, the flame spreads rapidly along the wall of the reflector, not only at the apex of the wedge. At 1.45 ms a flame kernel appears near the middle of the view field, leading to the formation of a detonation wave which propagates over the region in all directions.

Figure 5 depicts SIM and shows the sequence of events leading to detonation due to the interaction of oblique shock waves in 35% H2 in air mixture. The incident shock wave traveling initially at V_{refl} =714.88 m/s is reflected as the shock collides with the inner wall of the wedge and ignites through the apex of the wedge at 0.855 ms. At 0.870 ms, the flame has coupled and propagated with the second shock wave, and at 0.895 ms, it merges with the first reflected shock wave. The coupling propagation velocity is 1829.30 m/s with respect to the tube walls at 0.905 ms. However, the detonation propagates in a shocked gas being in motion and the axial velocity of the shocked gas is 396.66 m/s (calculated with Gaseq software). These values result in a coupled wave propagation velocity of 2225.96 m/s, leading to the formation of a detonation. The ideal CJ detonation for such mixture is 2076.59 m/s, which suggests an initially overdriven detonation.

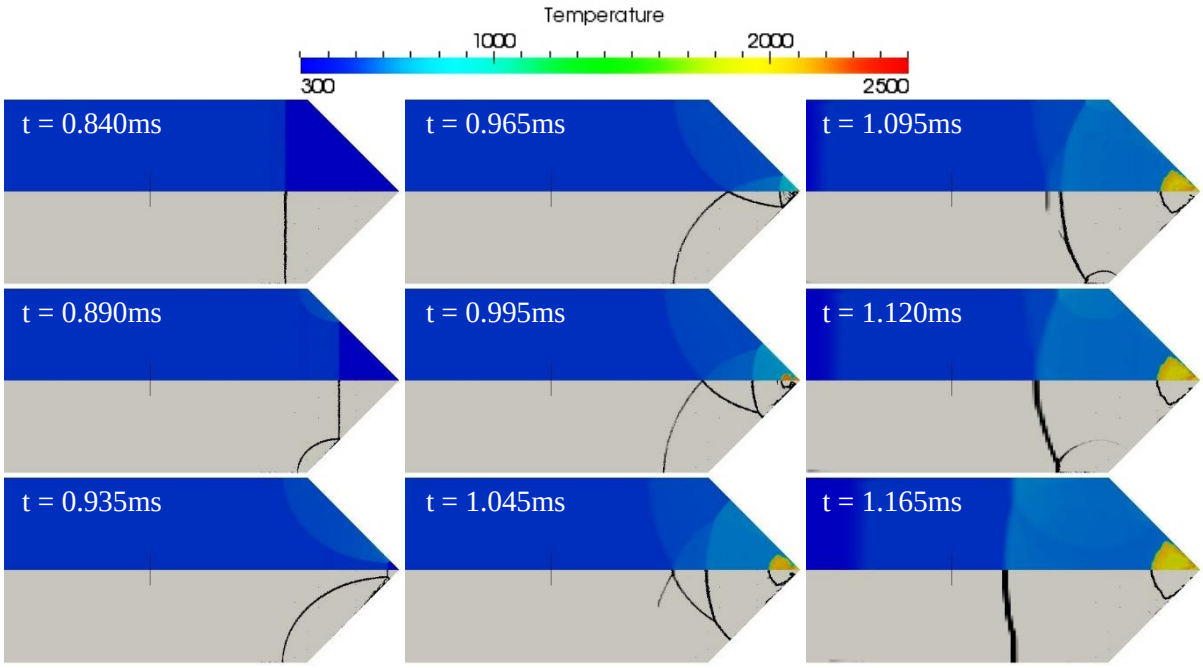

Figure 3. Temperature distribution (upper half) and shadowgraph (lower half) of the numerical simulation for the peak local ignition mode for 20% H_2+air mixture and V_{refl} = 643.7 m/s.

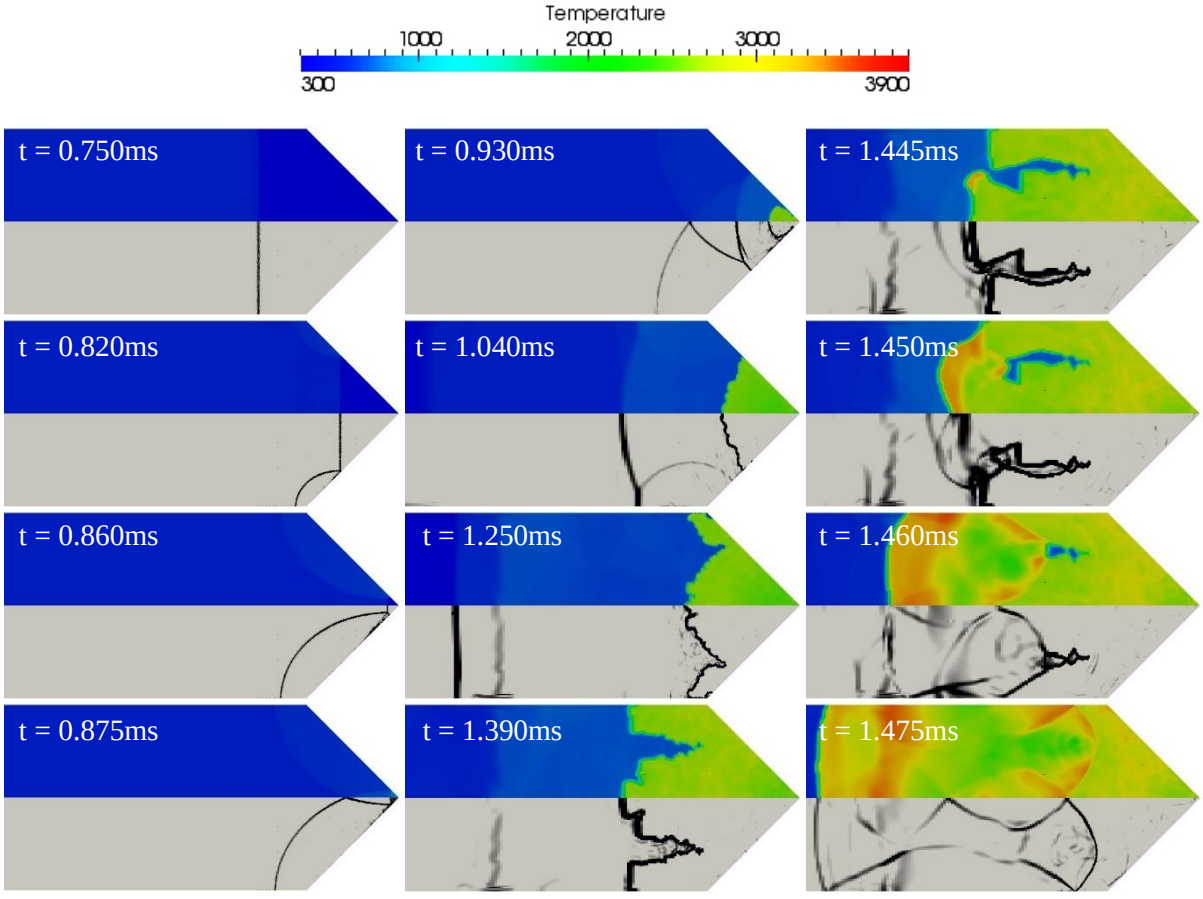

Figure 4. Temperature distribution (upper half) and shadowgraph (lower half) of the numerical simulation for the boundary ignition mode for 35% H_2+air mixture and V_{refl} = 698.65 m/s.

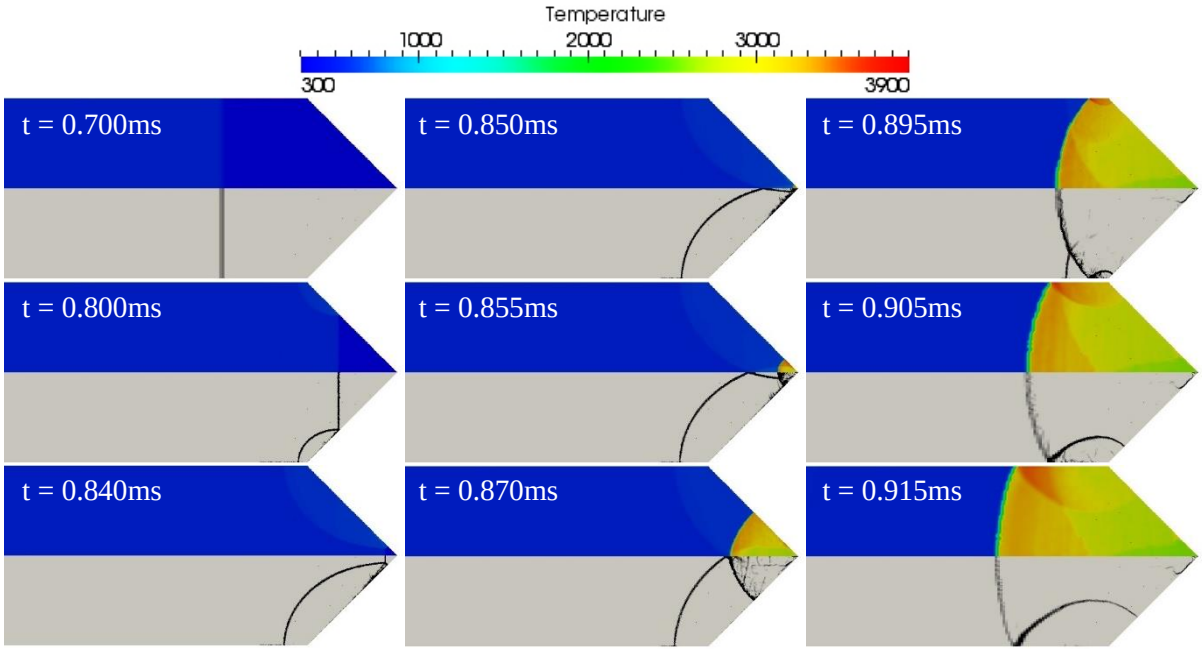

Figure 5. Temperature distribution (upper half) and shadowgraph (lower half) of the numerical simulation for the strong ignition mode for 35% H_2+air mixture and V_{refl} = 714.88 m/s.

Based on the results described above, it appears that the high intensity of pressure spikes from the pressure profile is a result of the occurrence of oblique shock waves at the point where reflected shock waves from the wedge-shaped wall intersect. Figures 6 to 8 illustrate examples of the pressure readings obtained from the pressure probes. The SIM (Fig. 8) exhibited a steeper pressure profile with higher maximal values than the PLIM (Fig. 6). The BIM (Fig. 7) had two pressure peaks recorded by PS5, with the second peak being 2 times higher (8.8 MPa) than the initial one, following a deflagrative ignition and delayed transition to detonation. Simultaneously, PS4 recorded approximately 2 times higher values compared to the first mode. This case is similar to observed in experiments where the transition to detonation occurred in the volume between PS4 and PS5. Similar observations were made by Buraczewski and Shepherd [6], where the transition distance from the reflector was highly sensitive to the initial shock wave velocity.

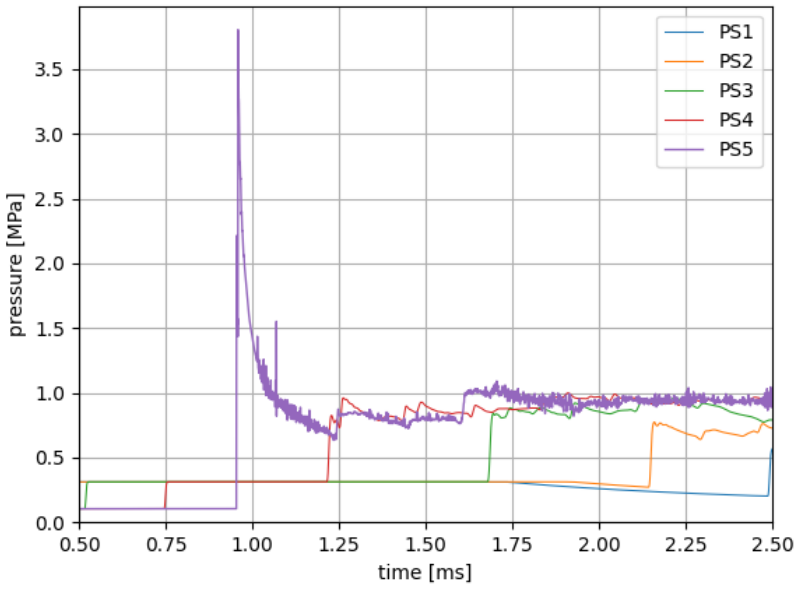

Figure 6. Pressure probes profiles for PLIM at 20% H_2+air mixture and V_{refl} = 643.7 m/s.

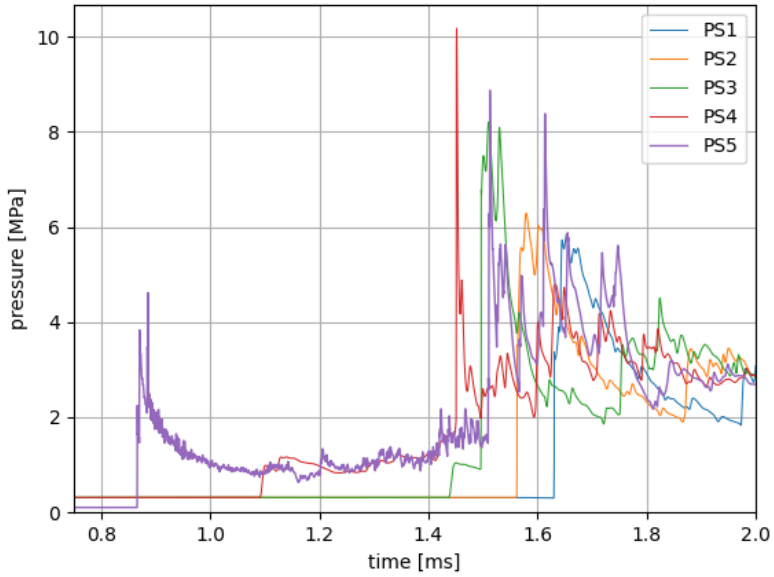

Figure 7. Pressure probes profiles for BIM at 35% H_2+air mixture and V_{refl} = 698.65 m/s.

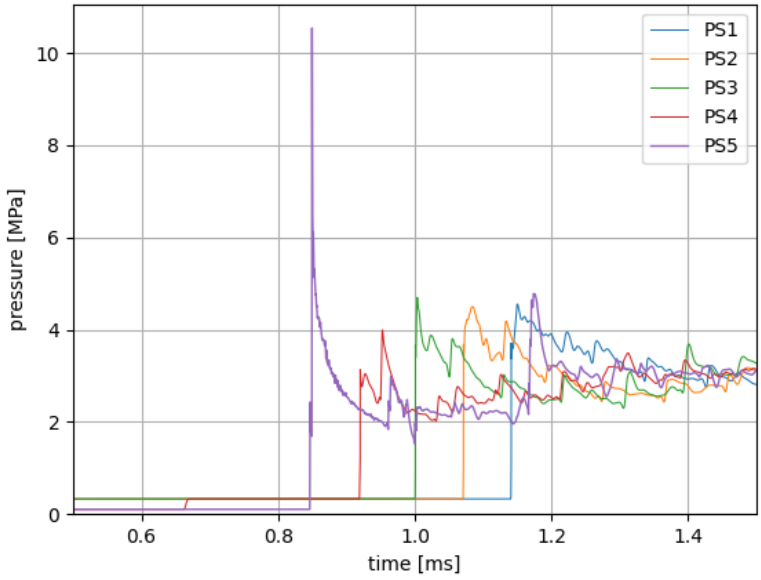

Figure 8. Pressure probes profiles for SIM at 35% H_2+air mixture and V_{refl} = 714.88 m/s.

The figures below illustrate the relationship between hydrogen concentration and the velocity of the leading shock wave as an absolute value (Fig. 9) and with respect to the speed of sound in the reactants (Fig. 10) and products (Fig. 11). Typically, the correlation for the transition to detonation limit follows a U-shape pattern with the lowest velocity values observed for near stoichiometric concentration. In the experimental investigation, the transition velocity for a 25% H_2 mixture was around 719 m/s, whereas in the numerical simulation, the transition velocity for the stoichiometric mixture was 663.83 m/s, corresponding to a Mach number of 1.67 and 70% of the speed of sound in products. This represents a 5.5% decrease in velocity compared to the experimental results obtained by Rudy [4]. The shock wave velocity must be increased more for lean or rich mixtures to observe the transition to detonation. Generally, the difference between the numerical and experimental data did not exceed 5-8% for mixtures containing around 25% to 45% hydrogen in air. However, the difference becomes more significant for leaner and richer mixtures, specifically H_2 < 25% and H_2 > 45% in air.

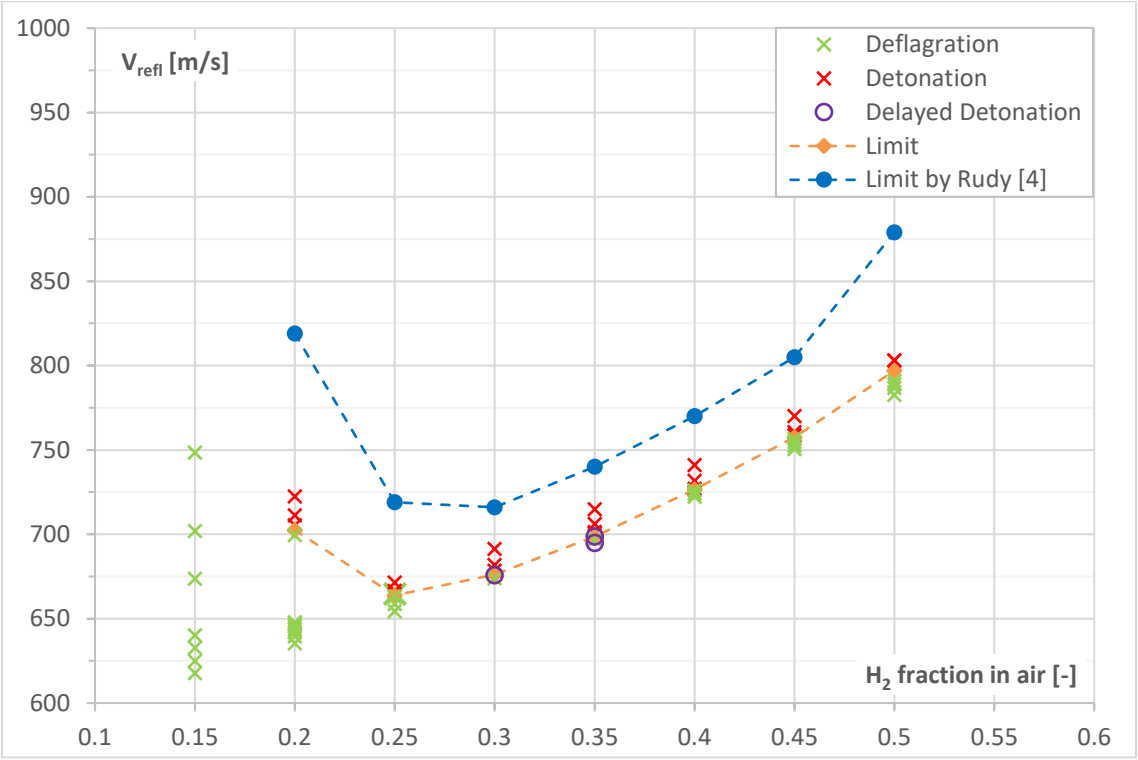

Figure 9. Shock velocity limit for transition to detonation in 90-deg wedge corner.

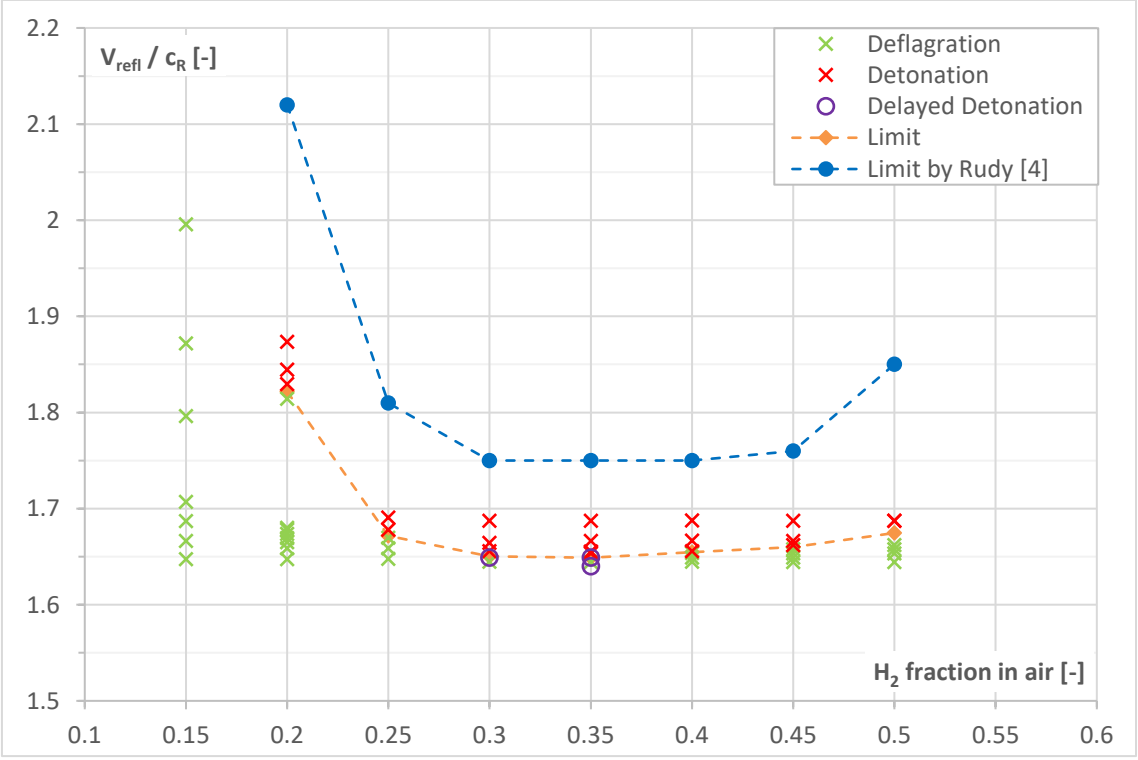

Figure 10. Velocity relative to speed of sound in reactants C_R limit for transition to detonation in 90-deg wedge corner.

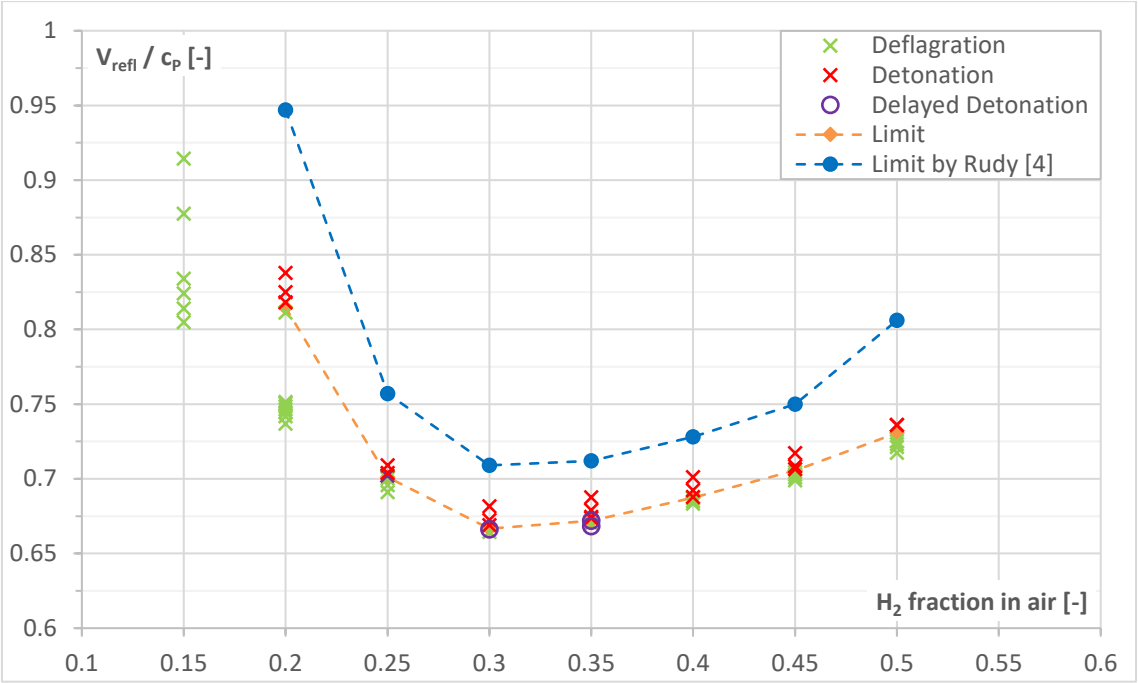

Figure 11. Velocity relative to speed of sound in combustion products C_P limit for transition to detonation in 90-deg wedge corner.

The summary graph of the maximum pressures recorded by Pressure sensor 5 is presented in Fig. 12. The limit line in Fig. 12 connects the points with an average value between the lowest recorded pressure of the detonation mode and the highest from the deflagration mode. The pressure in the corner required for direct detonation initiation is limited to a range of 7.9-9 MPa for 25%-50% H_2 in air, as shown by the limiting value from the experimental results. However, a deviation from this value has been observed, with a difference of about 10-36% for the numerical limit compared to the experimental limit. The largest differences were found for mixtures containing 35-40% hydrogen.

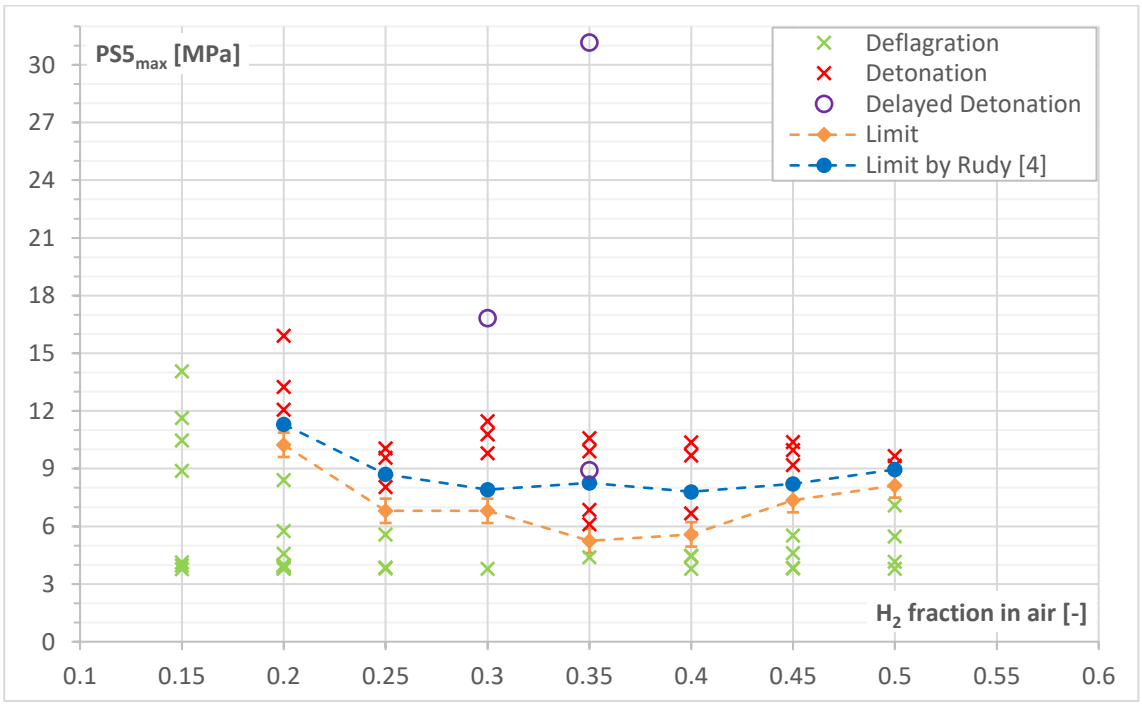

Figure 12. Summary graph of maximum pressure recorded by PS5 for all considered experiments.

The graphs in Figures 13 to 15 illustrate how the ignition delay time (IDT) is affected by the reflection velocity. The reflection velocity is a crucial factor in determining whether a detonation will occur. Higher reflection velocities result in increased pressure and temperature in the corner of the wedge, leading to a shorter ignition delay time and an increased likelihood of DDT. Therefore, there is generally a critical shock wave velocity beyond which DDT is more likely to occur. For mixtures 15-50% H_2 in air the influence of the shock velocity on the IDT is visible, however, there is still a discrepancy when compared to the experiments results, where the numerical outcomes reached higher values of IDT.

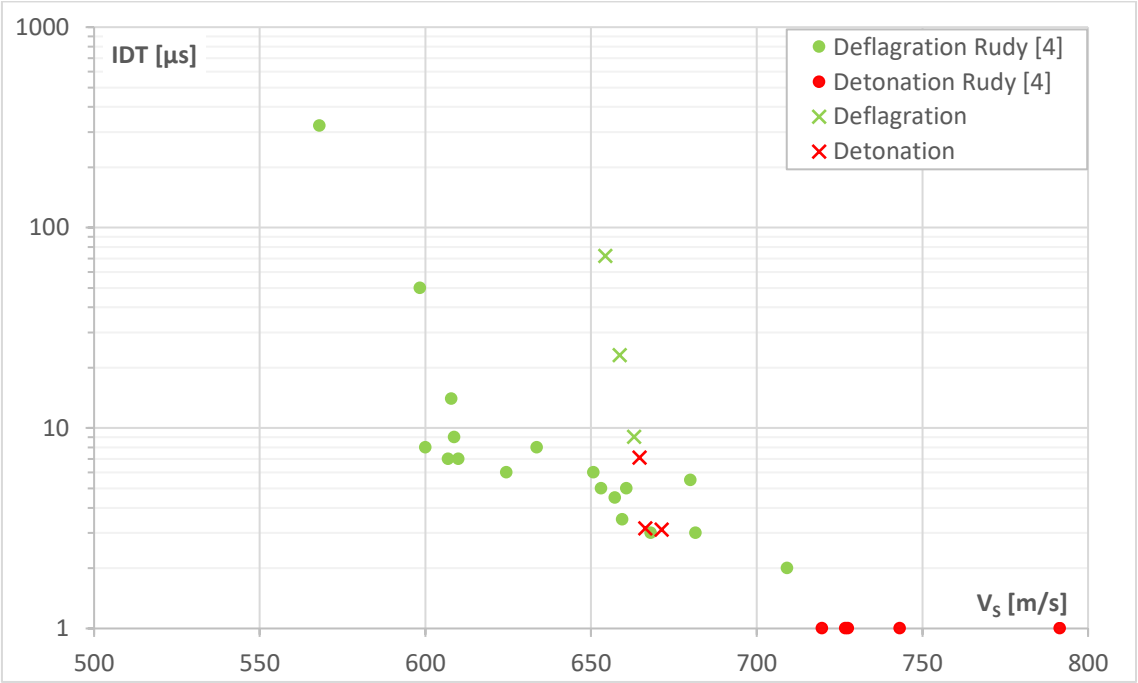

Figure 13. Ignition delay time in the corner as a function of reflection velocity for 25% H_2-air mixture.

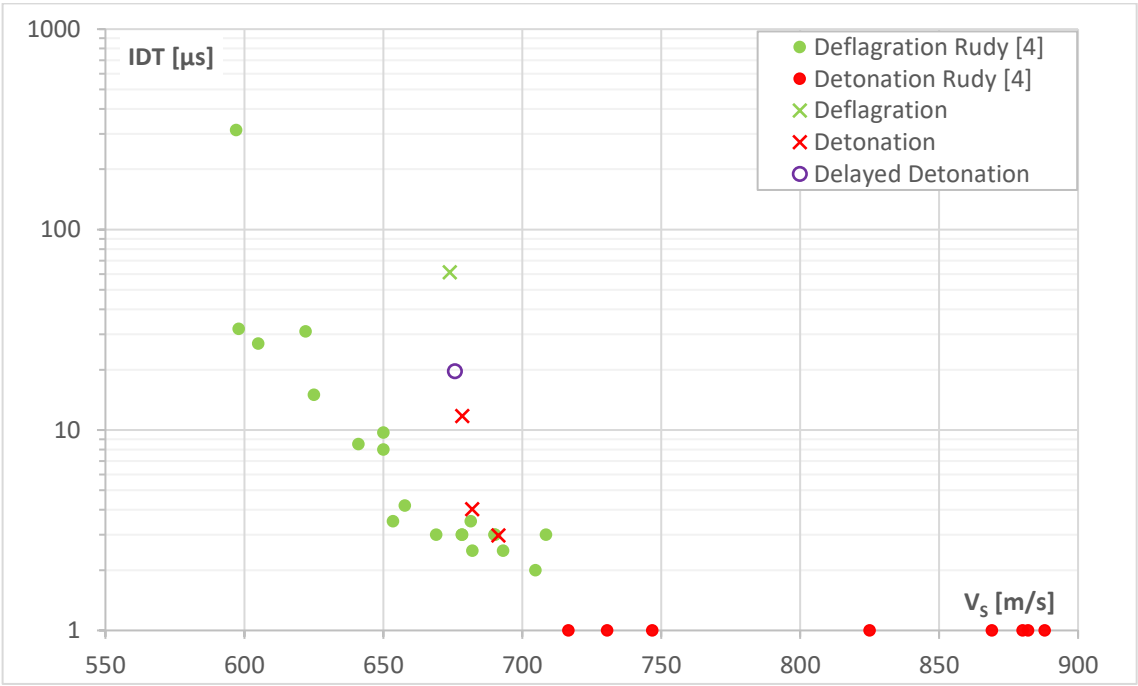

Figure 14. Ignition delay time in the corner as a function of reflection velocity for 30% H_2-air mixture.

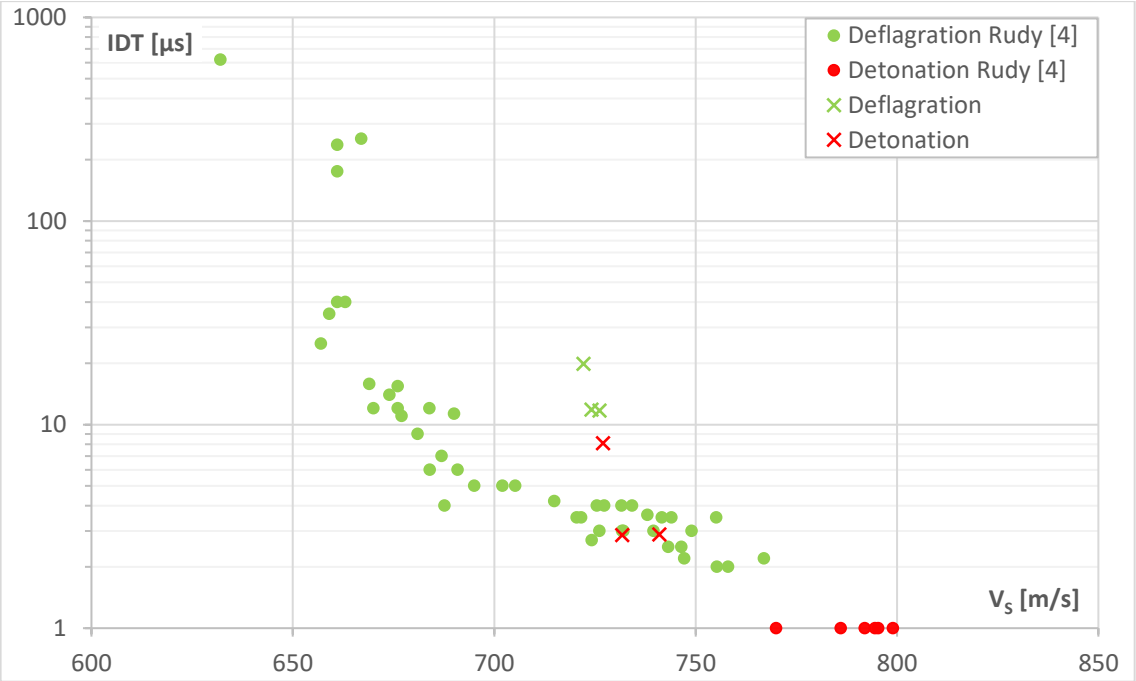

Figure 15. Ignition delay time in the corner as a function of reflection velocity for 40% H_2-air mixture.

5. CONCLUSIONS

The objective of this study was to use numerical simulations to replicate Rudy's [4] experiments and evaluate the ability of the ddtFoam code to predict DDT limits observed in those experiments. The numerical results showed three possible scenarios in the corner after focusing: deflagrative ignition in the corner, deflagrative ignition with intermediate transient regimes leading to a delayed transition to detonation in the lagging combustion zone at around 1.8 mm from the apex of the wedge, and ignition with an immediate transition to detonation, resulting in the formation of the detonation wave in the corner tip.

There was a discrepancy between the DDT limits obtained from numerical simulations and those observed in experiments. The transition velocity for the stoichiometric mixture was approximately 715 m/s in the experiments, while in the numerical simulations, the transition velocity was 675.65 m/s, indicating a decrease of 5.5% in velocity. In general, the difference in shock wave velocity was in range of 5-8%. The largest discrepancies were observed for the leaner and richer mixtures, specifically H2 < 25% and H2 > 45% in air, with differences of up to 15%. The likely cause of the nonconformity is the difference in the way of shock wave generation. However, the numerical results underestimate the critical shock wave velocity responsible for transition to detonation, which provides some level of safety margin while using ddtFoam for transition to detonation risk assessment.

6. REFERENCES

1. Ettner, F. A., Effiziente numerische Simulation des Deflagrations–Detonations–Übergangs, Doctoral Dissertation, Technischen Universität München, 2013.
2. Ettner, F. A., Sattelmayer, T., ddtFoam, 2013. [Online]. Available: https://sourceforge.net/projects/ddtfoam/
3. Ettner, F. A., Vollmer, K. G., Sattelmayer, T., Numerical simulation of the deflagration-to-detonation transition in inhomogeneous mixtures, *Journal of Combustion*, 2014, 2014, doi: 10.1155/2014/686347.
4. Rudy, W., Transition to detonation in a hydrogen-air mixtures due to shock wave focusing in the 90-deg corner, *International Journal of Hydrogen Energy*, 2023, doi:

10.1016/J.IJHYDENE.2022.12.240.

5. Wintenberger, E., Hornung, H. G., Shepherd, J. E., Detonation Initiation by Shock Focusing, GALCIT Report, No. FM 2001.00X, Pasadena, CA 91125, 2001. [Online]. Available: https://shepherd.caltech.edu/EDL/publications/reprints/GALCIT_report_FM2001-00X.pdf
6. Buraczewski, P. M., Shepherd, J. E., Initiation of Detonation by Shock Focusing, GALCIT Report, No. FM 2004.004, Pasadena, CA, 2004. [Online]. Available: https://shepherd.caltech.edu/EDL/publications/reprints/GALCIT_FM2004-004.pdf
7. Smirnov, N. N., Penyazkov, O. G., Sevrouk, K. L., Nikitin, V. F., Stamov, L. I., Tyurenkova, V. V., Detonation onset following shock wave focusing, *Acta Astronautica*, 135, Jun. 2017, pp. 114–130, doi: 10.1016/J.ACTAASTRO.2016.09.014.
8. Smirnov, N. N., Penyazkov, O. G., Sevrouk, K. L., Nikitin, V. F., Stamov, L. I., Tyurenkova, V. V., Onset of detonation in hydrogen-air mixtures due to shock wave reflection inside a combustion chamber, *Acta Astronautica*, 149, Aug. 2018, pp. 77–92, doi: 10.1016/J.ACTAASTRO.2018.05.024.
9. Smirnov, N. N., Nikitin, V. F., Stamov, L. I., Different scenarios of shock wave focusing inside a wedge-shaped cavity in hydrogen-air mixtures, *Aerospace Science and Technology*, 121, Feb. 2022, p. 107382, doi: 10.1016/J.AST.2022.107382.
10. Zhang, B., Li, Y., Liu, H., Analysis of the ignition induced by shock wave focusing equipped with conical and hemispherical reflectors, *Combustion and Flame*, 236, Feb. 2022, p. 111763, doi: 10.1016/J.COMBUSTFLAME.2021.111763.
11. Li, Y., Zhang, B., Visualization of ignition modes in methane-based mixture induced by shock wave focusing, *Combustion and Flame*, 247, Jan. 2023, p. 112491, doi: 10.1016/J.COMBUSTFLAME.2022.112491.
12. Yang, Z., Zhang, B., Numerical and experimental analysis of detonation induced by shock wave focusing, *Combustion and Flame*, 251, May 2023, p. 112691, doi: 10.1016/j.combustflame.2023.112691.
13. Toro, E. F., Spruce, M., Speares, W., Restoration of the contact surface in the HLL-Riemann solver, *Shock Waves*, 4, No. 1, Jul. 1994, pp. 25–34, doi: 10.1007/BF01414629/METRICS.
14. Issa, R. I., Solution of the implicitly discretised fluid flow equations by operator-splitting, *Journal of Computational Physics*, 62, No. 1, Jan. 1986, pp. 40–65, doi: 10.1016/0021-9991(86)90099-9.
15. Weller, H. G., Tabor, G., Gosman, A. D., Fureby, C., Application of a flame-wrinkling les combustion model to a turbulent mixing layer, *Symposium (International) on Combustion*, 27, No. 1, Jan. 1998, pp. 899–907, doi: 10.1016/S0082-0784(98)80487-6.
16. O'Conaire, M., Curran, H. J., Simmie, J. M., Pitz, W. J., Westbrook, C. K., A comprehensive modeling study of hydrogen oxidation, *International Journal of Chemical Kinetics*, 36, No. 11, 2004, pp. 603–622, doi: 10.1002/kin.20036.
17. Kee, R. J., Rupley, F. M., Miller, J. A., et al., The Chemkin Thermodynamic Data Base, Chemkin Collection, Release 3., San Diego, CA, Mar. 2000. doi: 10.2172/7073290.